5th International Conference on Experimental Fluid Mechanics ICEFM 2018 Munich
Munich, Germany, July 2-4, 2018

Influence of suction on step-induced boundary-layer transition

Benjamin Dimond[1*], Marco Costantini[1], Steffen Risius[1], Carsten Fuchs[1], Christian Klein[1]

[1] Deutsches Zentrum für Luft- und Raumfahrt e.V. (DLR), Institute of Aerodynamics and Flow Technology, Goettingen, Germany

[*] benjamin.dimond@dlr.de

Abstract

The influence of suction on step-induced boundary-layer transition has been experimentally investigated in the Cryogenic Ludwieg-Tube Goettingen at large chord Reynolds numbers (up to $16 \cdot 10^6$), Mach numbers from 0.35 to 0.77 and various stream wise pressure gradients by means of Temperature-Sensitive Paint (TSP). Surface imperfections, implemented as combination of gap and forward facing step, caused transition to occur at a location more upstream than in case of a smooth surface (i.e. without gap and step). It was found that suction, achieved passively by exploiting the pressure difference between upper and lower side of the model, induced a movement of transition to a more downstream location than on the smooth configuration at the same test conditions. Thus, the effect of suction was to even overcompensate the adverse effect of the combination of gap and forward-facing step on boundary-layer transition.

1 Introduction

Laminar flow technology is of great interest as it can significantly reduce wall shear stress and therefore fuel consumption of commercial aircraft as opposed to wings of conventional aircraft with predominantly turbulent flow. According to Robert (1992), almost 50% of all aerodynamic drag arises from friction, yielding a high possibility for fuel savings by maintaining the flow laminar over a significant portion of the wing surface. One method to delay boundary-layer transition and thus extend the area of laminar flow is an appropriate wing contour design (natural laminar flow - NLF), another method is by means of suction (laminar flow control - LFC). Former has been demonstrated to be a suitable technology for aerodynamic surfaces with zero to moderate sweep (sweep angle $\varphi \lesssim 20^\circ$ - Wagner et al. (1989); Schrauf (2005)) and is a practical reality for gliders and business jets as described in Schaber (2000) or Fujino et al. (2003). At larger sweep angles, however, LFC is required to achieve large laminar flow areas according to Braslow (1999), Wagner et al. (1989) or Schrauf (2005). As reported in Joslin (1998), flow control by means of suction has mainly been studied and tested with perforated plates providing an approximately continuous suction over a large region. Early studies, like those in the 1950s and 60s, also experimented with suction through slits and slots on a flat surface (see e.g. Kosin (1965) or Bushnell and Tuttle (1979)). Despite the promising results already achieved with laminar flow technology, its practical application remains challenging in the presence of surface imperfections at structural joints, such as gaps and/or steps, which are probably unavoidable on real aircrafts (Wagner et al. (1989)). The influence on boundary-layer transition due to surface imperfections has been investigated for example by Nenni and Gluyas (1966), Costantini (2016) and Perraud et al. (2004). Furthermore there have been several studies on the effect of suction on transition in the absence of steps (see e.g. the reviews in Bushnell and Tuttle (1979) and Braslow (1999)). However, the influence of suction on transition in the presence of steps has only been examined in two studies: Hahn and Pfenninger (1973) experimentally investigated the effect of suction through gaps (i.e. slits) downstream of a backward facing step at low Mach numbers ($Ma < 0.1$); numerical studies have been conducted to examine suction through a gap upstream of a forward-facing step by Zahn and Rist (2017) but only for one Mach number ($Ma = 0.6$). Both studies however, only examine cases with zero pressure gradient and without (or only negligible) variation of Ma. In contrast, this work focuses on the effect of suction through a gap directly upstream of a forward facing step for a wide range of Mach numbers, Reynolds numbers and pressure-gradients.

2 Experimental Setup

In the present work, systematic experimental studies have been conducted in the low-turbulence (momentum turbulence level $Tu_{pu} \sim 0.06\,\%$) Cryogenic Ludwieg-Tube Goettingen (DNW-KRG) at large chord Reynolds numbers ($3.5 - 16 \cdot 10^6$), Mach numbers from 0.35 to 0.77 and various stream wise pressure gradients. For latter, the Hartree parameter β_H, suggested in Meyer and Kleiser (1989), was used as dimensionless parameter (-0.03 $\leq \beta_H \leq$ 0.15 in this work). It was calculated using the linearly fitted pressure gradient between 0.4 and 0.9 chord length (the pressure gradient was essentially uniform in this region) and the pressure coefficient at $x_c = 0.65$. Figure 1 depicts the two-dimensional wind tunnel model used for the experiments, presented in Costantini et al. (2016). It was designed to achieve a large area of uniform pressure gradient along the model's chord on the model's upper side (Costantini (2016); Costantini et al. (2016); Risius et al. (2018)), which is the surface of interest in the present work. The upper side was coated with TSP for transition detection (Tropea et al. (2007)) - Formulation and optical setup was the same as in Costantini et al. (2016). An additional aft part was attached to the original model (see Figure 1 left) to reduce separation and thus minimize external disturbances to the boundary layer on the model's upper side as discussed in Risius et al. (2018). Shims were installed between the front and main part of the model to obtain sharp forward-facing steps at 35% of the model's chord length (Costantini (2016)). Along with a nominally smooth configuration (i.e. with a shim thickness resulting in a smooth surface without a step), two step heights (h = 30 μm and 60 μm) were investigated; the corresponding step Reynolds numbers were, for example, $Re_h = U_\infty h/\nu_\infty \sim 1200$ and $Re_h \sim 2400$ for a chord Reynolds number of $Re_c = 8 \cdot 10^6$ and Mach number $Ma = 0.65$, respectively. Here, U_∞ is the freestream velocity and ν_∞ is the freestream kinematic viscosity. In this work, the model configurations will be named "smooth", "step-1" (30 μm) and "step-2" (60 μm). For configurations with a step, the main part of the model was additionally displaced in the streamwise direction using alignment pins to obtain a gap width of $d_{gap} = 200$ μm upstream of the steps. As sketched in Figure 1, right, narrow shims were used as placeholders on the starboard side of the model, whereas a continuous shim was used on the port side. For the investigated test cases, the examined model cross section induces a larger pressure on the model's upper side than on the model's lower side. This pressure difference induces an internal flow (suction for the model's upper side) through the gap (slit) in the regions of the model starboard side where no shims are present. For comparison, the gap on the port half of the model did not allow passive suction due to continuous shim. In this way, the effect of the combination of a gap and a forward-facing step on boundary-layer transition could be examined simultaneously with and without suction through the gap.

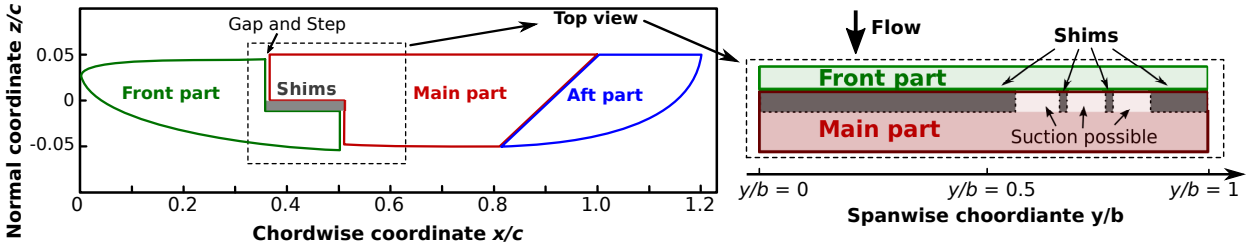

Figure 1: Simplified sketch of the wind tunnel model (chord length $c = 200$ mm, span $b = 500$ mm). The left sketch is a side view of the whole model cross-section, whereas the right sketch is a top view of the part highlighted by the dashed-lines rectangle. Shim sizes are in proportion, dimension of gap and step are enlarged for better visibility.

3 Results

Figure 2 depicts example TSP results obtained with the smooth (a), step-1 (b) and step-2 (c) configurations at Ma = 0.65, $Re_c = 8 \cdot 10^6$ and a favorable pressure gradient ($\beta_H \approx 0.07$). In the TSP results, bright areas correspond to laminar regions, whereas dark areas correspond to turbulent regions. Two turbulent wedges in the central area of the model can be observed, originating from pressure taps installed on the leading edge region. No TSP had been applied over the white strip visible in Figure 2: the junction between front and main part of the model is located in this region, which was left uncoated to enable the generation of sharp

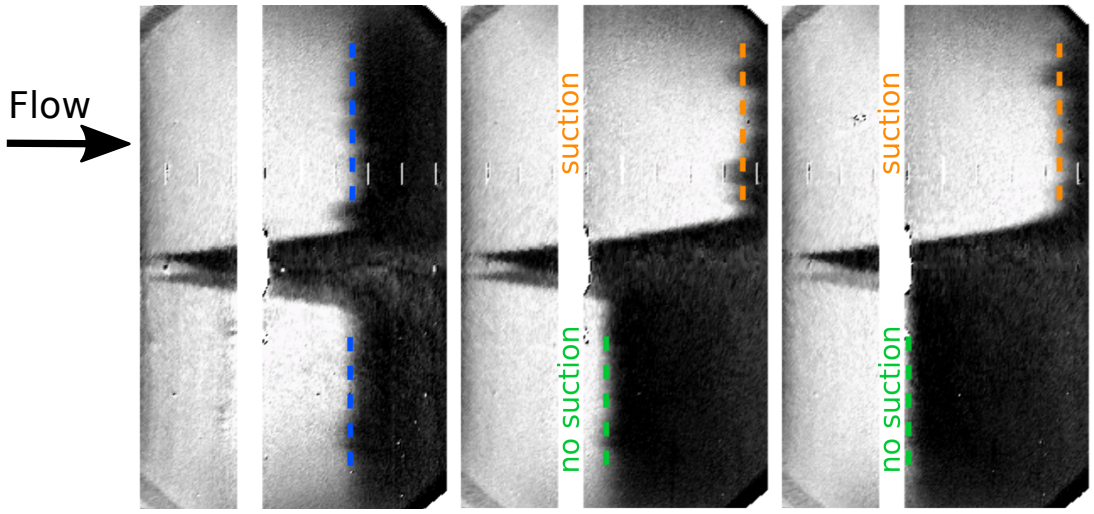

(a) smooth ($\mathrm{Re}_h \sim 0$) (b) step-1 ($\mathrm{Re}_h \sim 1200$) (c) step-2 ($\mathrm{Re}_h \sim 2400$)

Figure 2: TSP results for nominally smooth configuration (a) and step + gap configurations with $\mathrm{Re}_h \sim 1200$ (b) and $\mathrm{Re}_h \sim 2400$ (c) ($\mathrm{Re}_{\mathrm{gap}} = U_\infty d_{\mathrm{gap}}/\nu_\infty \sim 8000$ for both cases (b) and (c)). Transition was detected at $x_T/c \sim 65\%$ (blue) for (a), at $x_T/c \sim 45\%$ (green) and $x_T/c \sim 86\%$ (orange) for (b) and at $x_T/c \sim 40\%$ (green) and $x_T/c \sim 84\%$ (orange) for (c).

steps. Dashed lines indicate the detected, span-averaged transition location - blue for the smooth configuration, green for areas without suction and orange for areas with suction.
Without suction (port), the step and gap combination clearly induces a shift of the transition to a location more upstream than in the case of the smooth configuration. This effect is enhanced with a larger step height (c), in agreement to findings by Arnal (1992), Perraud et al. (2004) and Costantini (2016) for steps without gaps. For cases with suction (starboard), however, transition was shifted towards a more downstream location. It should be emphasized here that the suction effect overcompensates the adverse effect of combination of gap and forward-facing step, since transition was measured at a more downstream location than that detected on the smooth configuration. Interestingly, the effect of step height has no measurable effect on the transition location for cases with suction. In addition to that, note that the transition front is not as straight as without suction and appears frayed. These findings hold true for all conditions examined in the present work.

The results obtained with the smooth and step-2 configurations are collected in Figure 3a and 3b, respectively. Here, the transition Reynolds number $Re_{xT} = x_T U_\infty/\nu_\infty$ (formed with the detected transition location x_T) is plotted against the Hartree parameter β_H. It can clearly be seen that larger Re_{xT} were obtained by means of suction upstream of the forward-facing step, as compared to the smooth configuration. Note also that larger β_H lead to larger Re_{xT}. For the examined range of pressure gradients, however, the variation in Re_{xT} for a certain variation in β_H is larger with the smooth configuration than with the step-2 configuration with suction, suggesting that the dependency on the pressure gradient is not as high as for the smooth configuration. One further aspect is observable considering the effect of the Mach number. In contrast to the expectation based on linear stability theory (see Schlichting and Gersten (2000)) that larger subsonic Mach numbers stabilize the boundary layer, it seems that in this case lower Mach numbers lead to transition delay. As reported in Risius et al. (2018), this is probably due to the turbulence level in DNW-KRG which increases significantly with rising Mach numbers (Koch (2004)). When considering constant Mach number and Hartree parameter, the small variations in transition Reynolds number are caused by varying chord Reynolds number. This aspect was also investigated in Risius et al. (2018). It was found that transition for high chord Reynolds numbers was caused by Tollmien-Schlichting waves with higher frequencies than for low chord Reynolds numbers, and the initial turbulence level in DNW-KRG is lower for high frequencies. This effect is more significant in the reference configuration.

Figure 4 shows the transition Reynolds number Re_{xT} in dependency of the Hartree parameter β_H with a fixed Mach number (0.6) and chord Reynolds number ($8 \cdot 10^6$) for the different step heights with and without suction. Underlying TSP results for the step-1 configuration and three different pressure gradients

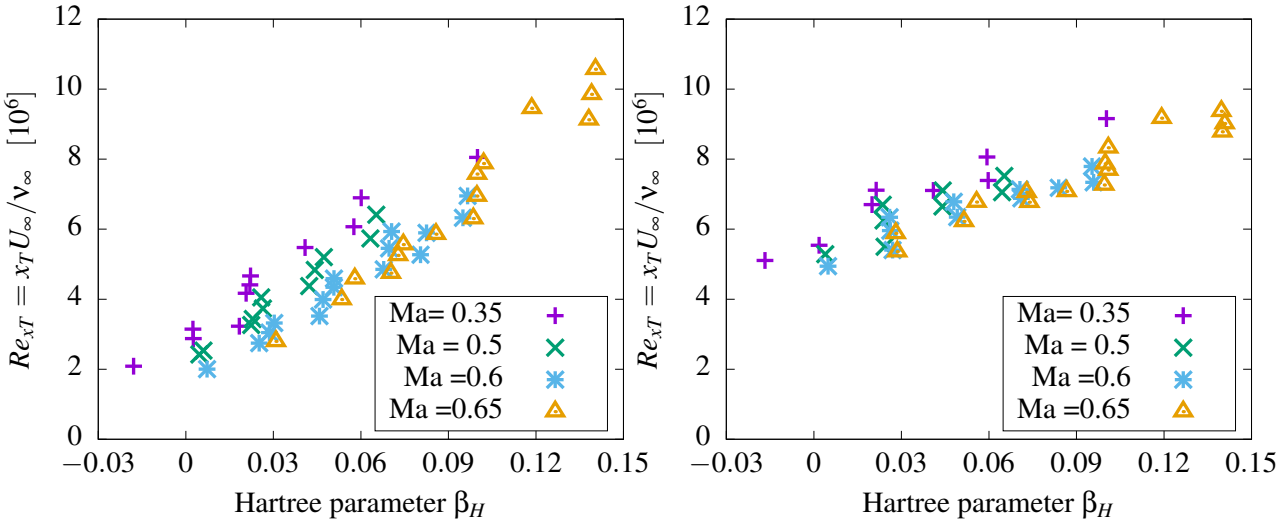

(a) smooth configuration

(b) large forward-facing step

Figure 3: Transition Reynolds number Re_{xT} as function of the Hartree parameter β_H. Error bars are typically smaller than the symbols and therefore not shown here.

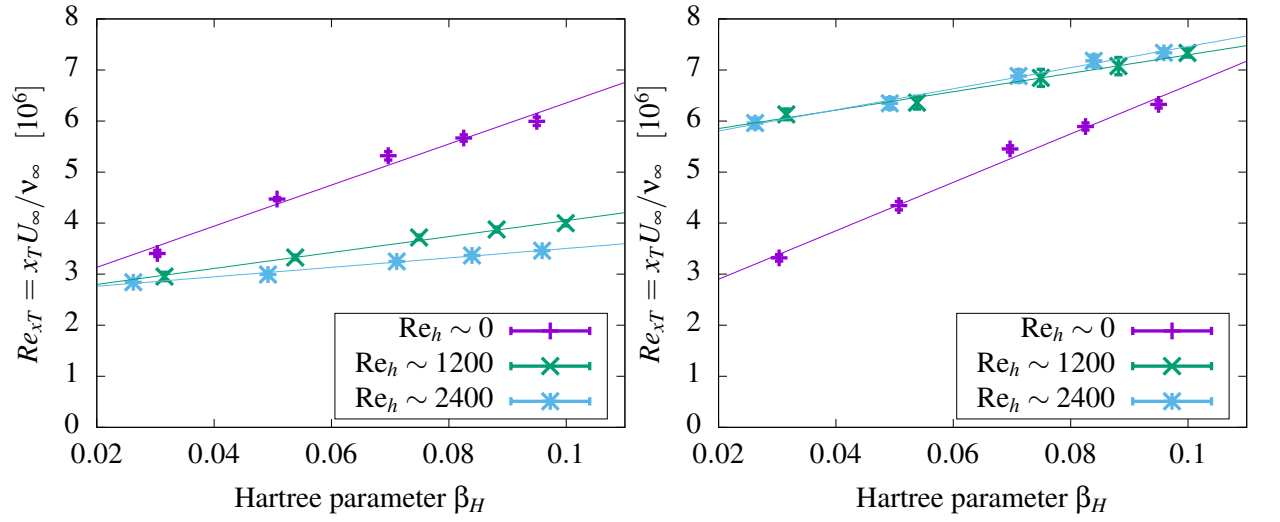

(a) Without suction (port).

(b) With suction (starboard).

Figure 4: Transition Reynolds number Re_{xT} as function of the Hartree parameter β_H for chord Reynolds number $Re_c = 8 \cdot 10^6$ and Mach number Ma = 0.6.

are depicted in Figure 5. The data in Figure 4 suggests a linear dependency within the examined Hartree-parameter range and thus a linear regression was plotted to guide the eye. Whereas without suction there is a difference of Re_{xT} for the two step heights at same Hartree parameter β_H, the cases with suction yield the same Re_{xT} for both step heights within the error range. This also holds true for all other examined Mach and Reynolds numbers. An explanation could be found in the relatively high suction rate: estimations of the suction velocity based on the pressure difference between upper and lower side of the model (driving force for suction) yield a relative velocity $v_{suction}/U_\infty$ between 0.2 and 0.3. This corresponds to a dimensionless suction rate $q = \dot{m}_s/\delta^*$ (with $\dot{m}_s$ being the massflow and δ^* the displacement thickness) of $q \gtrsim 1$ which is significantly larger than the suction range examined by Zahn and Rist (2017) of $q = 0.1$ and 0.3 in numerical studies or Hahn and Pfenninger (1973) for an experimentally investigated backward facing step of $q \lesssim 0.2$.

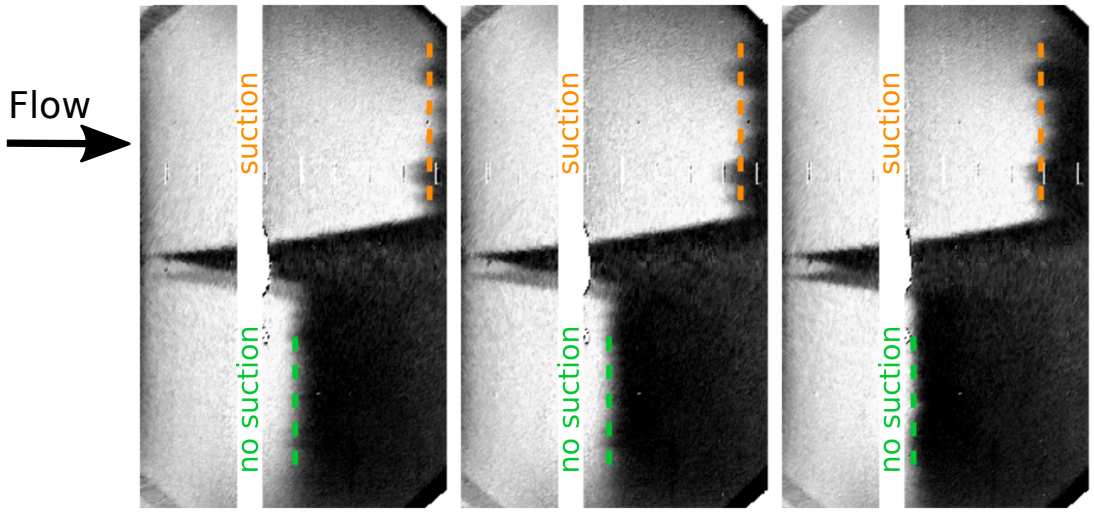

(a) $\beta_H = 0.088$ (b) $\beta_H = 0.075$ (c) $\beta_H = 0.054$

Figure 5: TSP results for step-1 (30 μm) configuration at different pressure gradients with chord Reynolds number $Re = 8 \cdot 10^6$ and Mach number $Ma = 0.6$ ($\mathrm{Re}_{gap} = U_\infty d_{gap}/\nu_\infty \sim 8000$ for all cases). Transition was detected at $x_T/c \sim 48\%$ (green) and $x_T/c \sim 88\%$ (orange) for (a), at $x_T/c \sim 46\%$ (green) and $x_T/c \sim 85\%$ (orange) for (b) and at $x_T/c \sim 41\%$ (green) and $x_T/c \sim 79\%$ (orange) for (c).

The interpretation of q as reduction of displacement thickness (which here is larger than the examined step heights) provides a possible explanation why the step height has no significant influence on transition location for cases with (high) suction.

4 Conclusion

Experimental investigations were conducted in the Cryogenic Ludwieg-Tube Goettingen to analyze the effect of suction on step-induced boundary-layer transition. Transition was detected by means of temperature-sensitive paint on a flat-plate model in a two-dimensional flow. Mach numbers ranging from Ma = 0.35 to 0.77 and chord Reynolds numbers from $\mathrm{Re} = 3.5 \cdot 10^6$ to $16 \cdot 10^6$ along with various pressure gradients were examined for two different step heights downstream of a gap with and without suction. Suction was achieved passively by a pressure difference between upper and lower side driving an internal flow. The combination of step and gap causes transition to occur further upstream, whereas suction through the gap was found to have a significant transition-delaying effect. This was to even overcompensate the adverse effect of the step and gap for the examined conditions. In the presence of suction, the effect of a variation in step height on transition seems to be negligible. Furthermore, the dependency of transition Reynolds number on the Hartree parameter β_H is significantly lower for step configurations (with and without suction) compared to the smooth configuration. The results obtained in the present work demonstrates that suction is a powerful tool for transition delay even in the presence of forward-facing steps.

Acknowledgements

The authors would like to thank M.Rein (DLR) for the valuable advice during the discussion of the results, A.Kunis (DLR) for the support during model modification, U.Henne (DLR) for the support of the TSP data analysis and V.Ondrus (University of Hohenheim) for the TSP development and synthesis. Furthermore, R.Kahle, M.Aschoff, A.Grimme and S.Hucke (DNW) are acknowledged for support during the measurement campaign at DNW-KRG.

References

Arnal D (1992) Laminar-turbulent transition. *Computational Methods in Hypersonic Aerodynamics* pages 233–264

Braslow AL (1999) *A history of suction-type laminar-flow control with emphasis on flight research*. No. 13. Monographs in Aerospace History

Bushnell DM and Tuttle MH (1979) Survey and bibliography on attainment of laminar flow control in air using pressure gradient and suction, volume 1. *NASA RP 1035*

Costantini M (2016) *Experimental Analysis of Geometric, Pressure Gradient and Surface Temperature Effects on Boundary-Layer Transition in Compressible High Reynolds Number Flows*. Ph.D. thesis. RWTH Aachen

Costantini M, Hein S, Henne U, Klein C, Koch S, Schojda L, Ondrus V, and Schröder W (2016) Pressure gradient and nonadiabatic surface effects on boundary layer transition. *AIAA Journal* pages 3465–3480

Fujino M, Yoshizaki Y, and Kawamura Y (2003) Natural-laminar-flow airfoil development for a lightweight business jet. *Journal of Aircraft* 40:609–615

Hahn M and Pfenninger W (1973) Prevention of transition over a backward step by suction. *Journal of Aircraft* 10:618–622

Joslin RD (1998) Aircraft laminar flow control. *Annual review of fluid mechanics* 30:1–29

Koch S (2004) *Zeitliche und räumliche Turbulenzentwicklung in einem Rohrwindkanal und deren Einfluss auf die Transition an Profilmodellen.*. Ph.D. thesis. Institute of Aerodynamics and Flow Technology, DLR Goettingen

Kosin RE (1965) Laminar flow control by suction as applied to the x-21a airplane. *Journal of Aircraft* 2:384–390

Meyer F and Kleiser L (1989) Numerical investigation of transition in 3d boundary layers. *Fluid Dynamics of Three-Dimensional Turbulent Shear Flows and Transition* page 16

Nenni JP and Gluyas GL (1966) Aerodynamic design and analysis of an lfc surface. *Astronautics & Aeronautics* 4:52

Perraud J, Arnal D, Seraudie A, and Tran D (2004) Laminar-turbulent transition on aerodynamic surfaces with imperfections. *RTO-AVT-111* pages 14–1 to 14–14

Risius S, Costantini M, Hein S, Koch S, and Klein C (2018) Experimental investigation of mach number and pressure gradient effects on boundary layer transition in two-dimensional flow. in *New Results in Numerical and Experimental Fluid Mechanics XI*. pages 305–314. Springer

Robert J (1992) Drag reduction: an industrial challenge. Technical report. AGARD-R-786-2

Schaber S (2000) *Auswirkungen von Schall und Absaugeverteilungen auf die Einsatzfähigkeit der Hybridlaminartechnik*. Ph.D. thesis. TU Berlin

Schlichting H and Gersten K (2000) *Boundary-layer theory, Chap 15: Onset of Turbulence (Stability Theory)*. Springer, Berlin. 8th edition edition

Schrauf G (2005) Status and perspectives of laminar flow. *The aeronautical journal* 109:639–644

Tropea C, Yarin AL, and Foss J (2007) *Springer handbook of experimental fluid mechanics, Chap. 7.4: transition detection by temperature-sensitive paint*. Springer Science & Business Media

Wagner R, Bartlett D, and Collier F JR (1989) Laminar flow-the past, present, and prospects. in *2nd Shear Flow Conference*. page 989

Zahn J and Rist U (2017) Active and natural suction at forward-facing steps for delaying laminar–turbulent transition. *AIAA Journal* 55:1343–1354